Int. J. Solids Structures Vol. 17, pp. 93–105
0020-7683/81/0101-0093/$02.00/0

AN UPPER-BOUND ON J FOR A CRACKED INFINITE PLATE MADE OF WHOLLY NON-LINEAR MATERIAL

T. G. F. GRAY
University of Strathclyde, Montrose Street, Glasgow, Scotland

(*Received 26 September 1979; in revised form 25 Feburuary 1980*)

Abstract—An approximate solution is provided for an internally cracked plate, loaded biaxially at infinity, where the material exhibits a wholly non-linear constitutive relation. The solution may be applied to plasticity problems where the applied stress is substantially above the limit of proportionality, or to stationary creep problems through the elastic analogy. The analysis leads to an upper bound on the value of J or $\dot{J}$, the path-independent line integral which is well-known in the field of fracture mechanics. Results are provided for a material following a simple n-power stress–strain or stress–strain-rate law and these are compared with another theoretical solution and experimental results taken from the literature.

INTRODUCTION

The underlying rationale of sharp-crack fracture mechanics is that various fracture phenomena which occur in real structures can be usefully described in terms of continuum mechanics models of idealised cracked bodies. The models should reflect the important features of the real situation such as the shape and size of the body including the crack, the loading, and the constitutive relation of the material. The importance of these and other features is usually established by a combination of experiment and experience. This paper is concerned with the modelling of wholly non-linear constitutive behaviour.

The first cracked body solutions in the literature were given for linear elastic materials. Later, solutions were provided which modelled yielding behaviour in a crack tip plastic zone where the material follows a non-linear law. A solution for a special shape of perfectly-plastic yield zone was provided by Dugdale[1] and results based on this model were given by Hayes and Williams[2] for finite plates loaded up to a stage where the plastic zone occupies the uncracked ligament completely. Detailed descriptions of the near-crack-tip stress distributions in work-hardening materials were given by Rice and Rosengren[3] and Hutchinson[4, 5].

In most solutions, the bulk of the body, situated between the plastic zone boundaries and the loaded surfaces, was assumed to remain in the linear elastic regime. In this paper, *all* of the material is assumed to be non-linear, the cracked body is in the form of a two-dimensional plate, loaded equibiaxially at infinity and the crack is non-propagating. In the analysis the material is deemed to be elastic, that is the work done by applied forces is a single valued function of the initial and final states of deformation and alternative plane strain and plane stress assumptions are followed through.

This model should be applicable in two main areas of fracture research. Firstly, to bodies made of conventional linear/elastic–plastic/work hardening materials where the loading is raised to gross stress levels above the limit of proportionality; secondly, to creeping materials which typically show a wholly non-linear stress–strain-*rate* constitutive behaviour. For the time-independent application it is envisaged that the strains due to non-linear response will be at all points in the body much larger than any linear elastic strains and the classical elasticity assumption restricts application to monotonically increasing loading and a deformation theory of plasticity. In the creep case the application will be to steady loading examples and any initial stress redistribution will not be described.

CHARACTERISATION OF CRACKING PROCESSES IN NON-LINEAR MATERIALS

The path-independent integral, designated J, [6] provides an appropriate characterisation for a material which is non-linear, at least in the crack-tip region. Whether J provides a unique description sufficient to form an adequate fracture criterion in all circumstances, is still worthy of examination, particularly in the case of stable crack growth. However, for the present purposes, these arguments may be set on one side and two analytical aspects of the J-integral noted—firstly, it anchors certain important features of the mechanical state at the crack-tip to the work input at the loaded boundaries (regardless of the constitutive relation of the intervening material) and secondly, J can be determined approximately by analyses which need not be exact in the near-crack-tip region.

The analysis of cracked bodies made of creeping materials is facilitated by the "elastic analogy". In this analogy, a solution for a material having a given instantaneous or quasi-static stress–strain law can be transferred to solve the same configuration of problem where the loading is steady and the material is creeping according to a stress–strain-*rate* law which is mathematically identical to the prototype stress–strain law. The stresses are the same in both materials (for identical loading) and the strains and displacements in the instantaneous solution transform to strain and displacement *rates* in the creep case. If we consider a load-specified elastic analysis for a crack problem where J can be defined as the change in complementary energy due to a vitural increase in crack surface area (see, e.g. Begley and Landes[8]), a solution for such a problem will also give $\dot{J}$ for the corresponding load-specified creep problem. ($\dot{J}$ can therefore be defined as the change in complementary power due to a virtual increase in crack surface area.)

It should not be readily assumed that $\dot{J}$ has necessarily any significance as a criterion for crack propagation or crack tip damage in creeping materials; rather it provides an analytical measure which allows estimates to be made of stress and accumulated strain and displacement in a creeping body at a non-propagating crack tip. The formulation of the integral is also sufficiently general to accomodate a material which is non-linear everywhere. These features of $\dot{J}$ were pointed out by Gildfind[9] and by Goldman and Hutchinson[10]. Nikbin *et al.*[11] also showed that recognition of the non-linear aspect in $\dot{J}$ calculations gave improved characterisation of creep-propagation experimental results.

Crack-tip-opening-displacement rates in creep may also be directly related to $\dot{J}$ through a creep analogue of the strip-yielding crack tip model. If the yield strength (also interpretable as the stress required to give infinite creep rate) is designated σ_y then the displacement rate $\dot{\delta}$ is given by

$$\dot{\delta} = \dot{J}/\sigma_y. \quad (1)$$

(The material surrounding the strip yielding zone need not be linear provided that $\dot{J}$ is correctly determined.)

Alternatively, it may be assumed that the restraining stress in the strip zone is related non-linearly at each point to the opening displacement rate of the zone. If the displacement rate at a given point in the strip zone is given by $\dot{\delta}(x)$ and the strain normal to the crack plane in the region of the zone is deemed to be distributed uniformly over a gauge length g (which may be related to plate thickness), then for a non-linear law in the strip zone of the type

$$\dot{\epsilon}/\dot{\epsilon}_0 = (\sigma/\sigma_0)^n \quad (2q$$

where $\dot{\epsilon}_0$ and σ_0 are suitably chosen constants, it can be shown that

$$\dot{J} = \int_0^{\dot{\delta}} \sigma_0[\dot{\delta}(x)/g\dot{\epsilon}_0]^{1/n}\, d\dot{\delta}(x)$$

whence

$$\dot{\delta} = \left(\frac{n+1}{n}\right)^{n/n+1} \frac{\dot{\epsilon}_0 g^{1/n+1}}{\sigma_0^{n/n+1}} \dot{J}^{n/n+1}. \quad (3)$$

(Clearly, removal of the dots will give the relationship for a non-linear work-hardening strip zone.)

BACKGROUND TO THE "DEAD-ZONE" ANALYTICAL MODEL

In an early attack on the problem of fracture mechanics application in the creep regime, Gildfind[9] carried out steady-load tests on cracked bodies made of thick lead-alloy plate. The cracks were non-propagating. It was hoped that an experimental study of the crack-tip-opening-displacement behaviour would assist understanding of the applicability of various analytical models available at that time. One important finding of the test series was that the stress/displacement-rate data could not be fitted to creep analogues of any of the elastic models available (e.g. the Dugdale Model); the reason being that the material did not exhibit a linear viscous element at low stresses, analogous to the linear elastic behaviour assumed for the bulk of the cracked body in time-independent solutions. It was clear therefore that the characterisation of creeping cracked bodies would require an appropriate non-linear analysis.

At that stage, desperate measures seemed justified, and recourse was made to a rudimentary treatment of the problem designated the "dead-zone model". This model is sometimes used in elementary text books where the authors wish to give a qualitative understanding of the Griffith concept for linear materials, while avoiding the complexities of a rigorous crack-tip stress analysis[13–15].

The model assumes that the stress state in a cracked body can be crudely described as in Fig. 1, in terms of a uniform uniaxial stress wverywhere in the body except in zone"sheltered" by the crack.

In this "dead" zone, the stress is supposed to be zero. The change in complementary energy or strain energy associated with the introducation of the crack is therefore given by

$$\bar{W} = -\frac{\sigma^2}{2E} \times (\text{area of dead zone}) \tag{4}$$

where E is Young's Modulus.

Of course, any shape of size of dead zone could be assumed, but it is clear that if the desired answer for a linear material is known in advance via more rigorous treatment, the area can be chosen to suit. Thus, for example, one might hypothesise an elliptical dead-zone shape with a major axis normal to the crack of $4a$. Hence

$$\bar{W} = -\frac{\sigma^2}{2E}\pi 2a^2$$

and

$$G = \frac{\mathrm{d}\bar{W}}{\mathrm{d}(2a)} = \sigma^2\pi a/E. \tag{5}$$

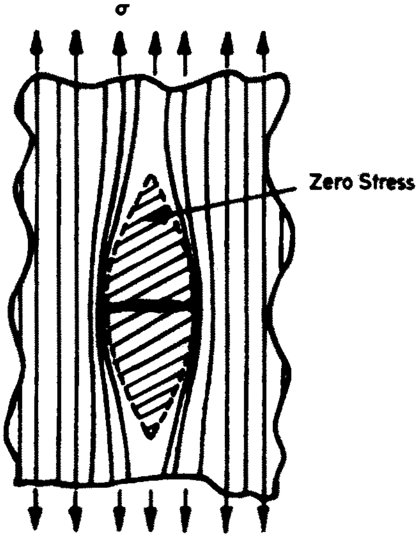

Fig. 1. Dead zone model.

(It should be noted that a *reduction* of complementary energy is implied by this treatment, whereas consideration of the load/displacement curves in a constant load compliance test would indicate an *increase* in energy.)

Using a non-linear constitutive law is hardly more difficult, except that one has to distinguish strain energy and complementary energy. Also, sadly, there is no convenient exact solution to guide the choice of dead zone area. For uniaxial loading and material which follows eqn (2), specific complementary energy $= (1/n+1)\cdot(\epsilon_0/\sigma_0{}^n)\cdot\sigma^{n+1}$. Retaining the elliptical dead zone shape, it was established that

$$G = \frac{1}{n+1}\frac{\epsilon_0}{\sigma_0{}^n}\sigma^{n+1}\pi a. \tag{6}$$

This model appeared to be dimensionally plausible and at least reflected the non-linearity of the material. As G determined in this way is equivalent to J, non-linear displacements or displacement-rates at the crack tip could be determined by path-independence, in the same way as the plastic zone in the linear case could be anchored to the small-scale yielding or Dugdale Model determination of J. Gildfind's major effort thereafter was directed towards testing the functional relationship, eqn (6), and its prediction of experimental crack-opening-displacements. This was carried out using work-hardening materials, loaded to gross stresses which corresponded to the limit of proportionality and upwards, thus simulating an entirely non-linear material. A dependence on σ^{n+1} was indeed established, but the magnitude of the proportionality constant in eqn (6) and/or its dependence on "n" or on other factors was not clearly shown.

AN ENERGY BOUND FOR THE DEAD-ZONE ANALYSIS

The dead-zone analysis may be improved by application of certain energy bound theorems (see, e.g. [16]). In particular, it can be shown from the principle of minimum complementary potential that for certain specified conditions the complementary energy associated with an approximate stress distribution is an upper bound on the true or exact complementary energy, that is

$$\int_{\text{vol}} \bar{W}(\sigma^*)\,\mathrm{d}v \geq \int_{\text{vol}} \bar{W}(\sigma)\,\mathrm{d}v \tag{7}$$

where $\bar{W}$ is complementary energy, (σ^*) denotes an approximate stress distribution which satisfies equilibrium internally and externally with the desired boundary tractions and (σ) denotes the true stress distribution. The problem must be entirely "load specified", that is, there should be *no* surfaces on which displacements are specified. The general method of solution is as follows:

1. Find a variable stress distribution which satisfies the differential equations of equilibrium internally and which is also in equilibrium with the specified surface tractions at the boundaries (including any boundaries where the tractions are zero).
2. Calculate the complementary term $\int_{\text{vol}} \bar{W}(\sigma^*)\,\mathrm{d}v$ associated with this distribution.
3. Vary the distribution until the minimum complementary energy is found.

The result will be an upper bound on the complementary energy. If the tractions are derived from a single load action, the structure associated with the optimised stress state will be *more flexible* than the real structure. The method can accept a wide variety of constitutive relations. Note also that since *any* equilibrium stress pattern may be used to form the approximate field, the stress field from a linear elastic solution could be employed whether or not the material is linear.

The status of the crude dead-zone model can now be defined—the approximate variable stress distribution in that model does not satisfy the differential equations of equilibrium at the perimeter of the dead zone. Therefore, although it satisfies the boundary conditions and it incorporates the correct constitutive relation, it cannot be shown to be a bound of any kind, nor can the shape of the dead zone be optimised. Specialising the energy procedure to cracked bodies, two further steps need to be added:

4. Subtract the complementary energy in an uncracked body of the same dimensions

loaded to the same boundary tractions and the energy associated with insertion of the crack is obtained.

5. Differentiate the remaining energy term with respect to crack length and J is obtained. However, it should be noted that the variational procedure as stated in Steps 1–5 will not in general ensure an upper bound on J. *Differential* energy quantities cannot normally be bounded, as there is no indication of how close to the exact state the optimised stress distribution is. Hence if the optimisation procedure is applied to two bodies which are slightly different in some way, say, e.g. the crack lengths are different, it is impossible to be certain which of the two energies is closer to its respective true state. It therefore cannot be determined whether the difference between the two energies in the approximate case is greater or less than true difference. Therefore if an upper bound on J is required, a further restriction on the minimisation procedure must be accepted, namely, that the crack length must be held constant during the energy minimisation. This in turn suggests that the approximate stress distribution should be set up in such a way that the crack length and the parameters which are to be varied are separate in the formulation, for example,

$$\sigma^* = f(\sigma, a, \lambda)$$

where λ is a variable parameter independent of a. Note also that in Step 4, the energy subtracted must be the *exact* energy in the uncracked body (or less).

We proceed by considering the linear-elastic stress distribution produced by a symmetrical cut-out which is matched to the crack length as shown in Fig. 2. The material within the hatched border is still present, but as there are no normal or shear tractions on the perimeter of the dead zone, there will be no stresses within it and therefore no complementary energy contribution. The model differs from the crude analysis, however, in that the stresses outside and on the dead-zone border satisfy the differential equations of equilibrium. Of course this distribution may bear only a passing resemblance to the real situation, but that circumstance does not prevent one from using it to form a valid upper bound.

The stress distribution may be altered by varying the shape and size of the dead-zone border. However by anchoring the zone to the ends of the crack, the necessary condition that the variable elements should be independent of crack length, is established.

FORMULATION OF THE SPECIFIC COMPLEMENTARY ENERGY

First, an "equivalent" or "effective" stress

$$\bar{\sigma} = \frac{1}{\sqrt{2}}[(\sigma_1 - \sigma_2)^2 + (\sigma_2 - \sigma_3)^2 + (\sigma_3 - \sigma_1)^2]^{1/2} \tag{8}$$

and a corresponding quantity "effective strain"

$$\bar{\epsilon} = \frac{\sqrt{2}}{3}[(\epsilon_1 - \epsilon_2)^2 + (\epsilon_2 - \epsilon_3)^2 + (\epsilon_3 - \epsilon_1)^2]^{1/2} \tag{9}$$

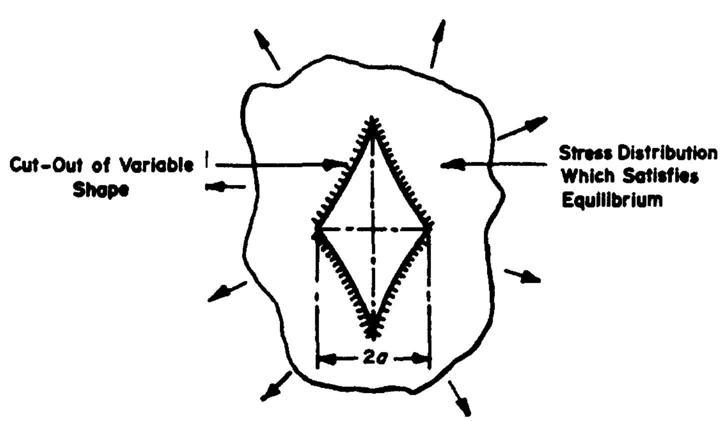

Fig. 2. Improved dead zone model.

are defined, where it is assumed that the strains combine to preserve constant volume ($\nu = \frac{1}{2}$). In the creep case, "effective strain rate" can be defined in identical fashion by placing dots above all strain terms. Also the relation

$$\frac{\bar{\epsilon}}{\epsilon_0} = \left(\frac{\bar{\sigma}}{\sigma_0}\right)^n \tag{10}$$

is assumed where ϵ_0 and σ_0 are corresponding values chosen at an arbitrary point on a stress–strain curve produced by a uniaxial test.

For steady state creep, the relationship (10) is realistic for many materials, although other relationships have been shown to be equally satisfactory. Finnie and Heller[17] also show that the relationship between principal stresses and strains (or strain rates) for such materials will be given by

$$\epsilon_1 = \frac{\epsilon_0 \bar{\sigma}^{n-1}}{\sigma_0^n}\left[\sigma_1 - \frac{1}{2}(\sigma_2 + \sigma_3)\right] \tag{11a}$$

$$\epsilon_2 = . \quad . \quad . \quad . \quad . \quad . \tag{11b}$$

$$\epsilon_3 = . \quad . \quad . \quad . \quad . \tag{11c}$$

allowing formulation of the specific complementary energy functions through the simultaneous integral

$$\bar{W}(\sigma) = \int_0^{\sigma_1, \sigma_2, \sigma_3} (\epsilon_1\,\mathrm{d}\sigma_1 + \epsilon_2\,\mathrm{d}\sigma_2 + \epsilon_3\,\mathrm{d}\sigma_3). \tag{12}$$

Equations (10)–(12) can be simplified by making the assumption of plane stress ($\sigma_3 = 0$) or plane strain ($\epsilon_2 = 0$).

To proceed further, a relationship between σ_1 and σ_2 must be established. In the present dead-zone model, the assumed stress distribution automatically determines that at each point in the material the principal stresses are in a fixed ratio and in any case "proportional" loading is commonly assumed[18]. (Note that the necessary conditions for proportional loading are not satisfied for the strip yielding model where the crack surface tractions do not increase in proportion to the externally applied load.) Inserting the condition $\sigma_1/\sigma_2 =$ constant therefore,

$$\bar{W}(\sigma) = \frac{\epsilon_0}{\sigma_0^n}\frac{1}{(n+1)}\bar{\sigma}^{n+1} \tag{13}$$

where

$$\bar{\sigma} \text{ plane stress} = (\sigma_1^2 + \sigma_2^2 - \sigma_1\sigma_2)^{1/2} \tag{14a}$$

$$\bar{\sigma} \text{ plane strain} = \frac{\sqrt{3}}{2}(\sigma_1^2 + \sigma_2^2 - 2\sigma_1\sigma_2)^{1/2}. \tag{14b}$$

AN APPROXIMATE STRESS FIELD

Following an initial unsuccessful attempt using an edge-notch solution due to Stevenson[19], the elliptical hole solution of Inglis[20] was used. In terms of the elliptical coordinate system uned by Inglis (see Fig. 3) and for biaxial loading, the complementary energy is given by

$$\int_{\mathrm{vol}} \bar{W}(\sigma^*)\,\mathrm{d}v = \frac{\epsilon_0}{\sigma_0^n}\frac{1}{(n+1)}\int_0^{2\pi}\int_0^{\xi_{\max}} [(\sigma_\xi + \sigma_\eta)^2 + |\sigma_\xi - \sigma_\eta + 2i\tau_{\eta\xi}|^2]^{n+1/2} h^2\,\mathrm{d}\eta\,\mathrm{d}\xi \tag{15}$$

(the term in square brackets being an alternative formulation of effective stress.)

Here ξ_0 defines the edge of the elliptic hole and consequently the shape of the dead zone,

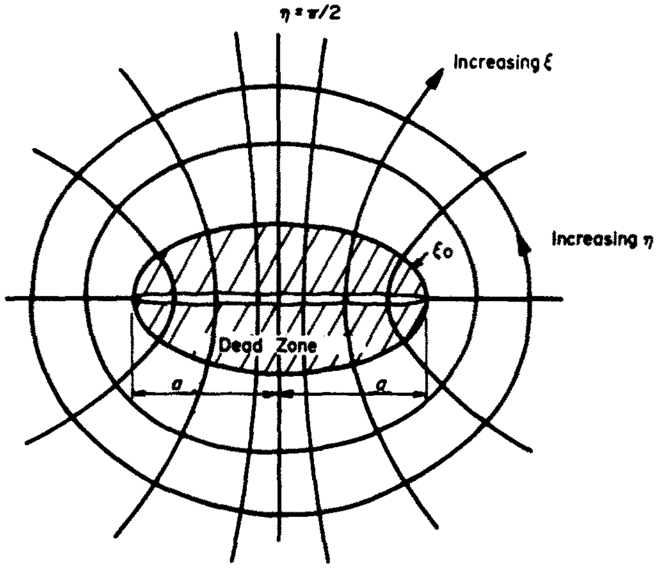

Fig. 3. Coord system for eqns (15)–(17) and (27).

i.e. ratio of minor to major axis, ξ_{max} is an arbitrary outer limit which gives a nearly circular boundary and "h" is a magnification factor required to transform the size of the element. The formulation of h and suitable stress functions for the terms in eqn (15) can be derived from (21) viz.

$$h^2 = a^2\left[\frac{\sinh^2\xi\cos^2\eta + \cosh^2\xi\sin^2\eta}{\cosh^2\xi_0}\right] \tag{16}$$

and for example

$$\sigma_\xi + \sigma_\eta = \sigma 2\sinh 2\xi/(\cosh 2\xi - \cos 2\eta). \tag{17}$$

It can be seen from these two equations that the applied stress σ and the "crack" length "a" can be extracted from the terms inside the integration sign and therefore the integral depends only on ξ_0 and ξ_{max}.

This derivation of the complementary energy in a plate with an elliptical hole differs from that of Griffith[22] in that the specific complementary energy term is integrated throughout the volume whereas Griffith integrated the work done by boundary tractions. However the result for linear elastic material is identical (within the accuracy of numerical integration procedures). Varying ξ_0 to produce minimum energy showed that for a linear-elastic material the minimum was found with a vanishingly narrow ellipse ($\xi_0 \to 0$) as expected, and led to the result

$$G = \nu\frac{\sigma^2\pi a}{E} \tag{18}$$

as given by Griffith in his 1921 paper. Of course this result is wrong; it merely repeats the error made by Griffith which was corrected later in 1924[23]. The basis of the modification which Griffith used to alter the boundary tractions and thereby produce the "correct" 1924 result was never published and as a consequence several authors discussed the error and others drew mistaken conclusions from the earlier incorrect solution. A clear exposition of the mistake and a possible correction route was given by Spencer[24].

The error arises in essence because the stresses in the Inglis solution at a large but not yet infinite distance from the hole edge differ from the required boundary traction by a small amount. Although the difference seems infinitesimal, the "error energy" is integrated over a large circuit. It should be noted that there is in fact *no* error in the determination of energy using this method. The problem only arises at Step 4 defined earlier where the change in energy due to introduction of the crack is found by subtracting the energy in a *finite* uncracked plate of the same dimensions loaded to the same boundary conditions. As this uncracked plate will exhibit a different boundary condition to the finite part of the infinite cracked plate, the subtraction is invalid.

The correction procedure adopted by Spencer and Sih and Liebowitz[24, 25] was to find additional stress functions which described a stress distribution in equilibrium with the *difference* between the stress given by Inglis' solution at a given large but finite radius and the desired boundary traction. The stresses derived from this correction term could then be added to the Inglis terms to give the required complete solution. The required correction terms for an arbitrary elliptical hole in a finite plate subject to a biaxial stress are given in the Appendix. (The formulation has been transformed from the polar coordinates of [25] which are useful only at the large outer boundary, to elliptical coordinates which can be readily applied throughout the body.)

Even this stress correction is incomplete, as there remains a small stress of order $(a/R)^2$ normal to the elliptical hole boundary (where R is the large radius outer boundary). This error did not affect Spencer's result because the work integration was carried out on a circuit around the outer boundary where the displacements were negligibly influenced by the discrepancy. However it was considered possible that such an error might be more significant in non-linear energy calculations where the corrections are raised to the power $(n+1)$. Therefore to secure confidence that the final result would be a true upper bound, eqns (27) and (28) were applied a second time to neutralise the edge-of-hole error. (The resulting error in the outer boundary would then be $(a/R)^4$.) As a final check, the composite stress distribution produced by these superpositions was evaluated for a finite plate of outside radius 75 times the larger dimension of the cut-out, which was varied between a sharp crack and a circular hole. The boundary traction errors (inner and outer) were always less than order $(a/R)^4$ and similar accuracies were proved throughout the field for the circular hole case by comparison with the classical Lamé equations.

RESULTS FOR NON LINEAR MATERIALS

To apply the method to non-linear materials, a specific value of n was chosen and the composite stress field was fed into the numerical integration procedure used to evaluate eqn (15)

$$\dot{J} = \frac{\mathrm{d}}{\mathrm{d}a}\left[\int_{\text{cracked plate}} \bar{W}(\sigma^*)\,\mathrm{d}v - \int_{\text{uncracked plate}} \bar{W}(\sigma)\,\mathrm{d}v\right]. \tag{19}$$

The boundary ξ_0 was varied until a minimum energy was obtained. ξ_{max} was also varied with cut-out shape to secure an approximately constant outer radius of 75 times the half-crack-length. (As the external boundary shape changes slightly with cut-out shape, ξ_{max} was altered to give a constant *area* of uncracked plate.)

To check the integration accuracy, "energy release rates" for a 1/1000 elliptical hole and a circular hole under plane strain and plane stress conditions were compared with Griffith's 1924 result for a sharp crack and with an analytical integration of the Lamé distribution for a circular hole. The results all checked to less than 0.1%. The procedure was then repeated for several values of n between 0.1 and 14 corresponding to different materials.

It should be noted that from eqn (15) it would be a relatively simple matter to run the program for different constitutive laws as long as the specific complementary energy under biaxial loading can be cast in the form $\bar{W}(\sigma) = f(\bar{\sigma})$. This condition may be satisfied for some double-power creep laws, for example, and for time-hardening laws.

In the plane stress case, the shape of the optimised dead zone changed monotonically with n from a vanishingly flat ellipse as $n \to 0$ to a circular zone as n tended to infinity. In the plane strain case, a flat elliptical zone was found for all values below $n = 1.8$ and above this value the shape tended towards the previous circular limit.

Finally, the energy associated with an uncracked uniformly loaded plate of the same area was subtracted and $\dot{J}$ was found from the relationship eqn (19).

The results can be expressed in a number of ways. In Fig. 4, $\dot{J}$ is non-dimensionalised for

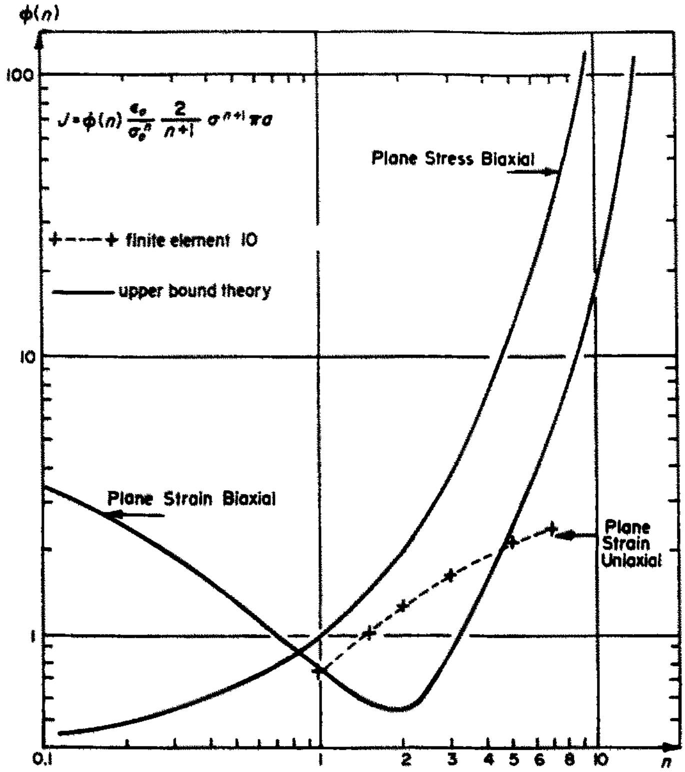

Fig. 4. $\dot{J}$ characterisation of an infinite 2-D body made of wholly non-linear material.

time-dependent non-linear material in the form

$$\dot{J}=\phi(n)\frac{\dot{\epsilon}_0}{\sigma_0{}^n}\frac{2}{(n+1)}\sigma^{n+1}\pi a \tag{20}$$

this being a form which reduces to $\sigma^2\pi a/E$ when $n=1$ and $\sigma_0{}^n/\dot{\epsilon}_0=E$. Note also that in the plane strain case the factor $(1-\nu^2)$ is included in $\phi(n)$, where $\nu=\frac{1}{2}$.

The cross-over of the plane–strain and plane–stress results seemed anomalous, although some of the initial drop in the plane strain results is accounted for by the plane–strain factor $(\sqrt{3}/2)^{n+1}$ (see eqns 13 and 14). Numerous checks using different external radii and integration routines were made and no numerical errors were revealed.

Alternatively, the crack-opening-displacement rate (or crack-opening displacement for time-independent material) may be related to the results by combining eqns (3) and (20), viz.

$$\dot{\delta}=(2/n)^{n/(n+1)}g^{1/(n+1)}\frac{\dot{\epsilon}_0}{\sigma_0{}^n}\sigma^n(\pi a)^{n/(n+1)}[\phi(n)]^{n/(n+1)}. \tag{21}$$

This equation is based on a model where the near-crack-tip plastic strain is concentrated in a strip. The closing forces in this strip are related to the separations by the same non-linear law as assumed for the bulk of the material. The strip zone is therefore embedded in a field of non-linear material which extends to the loaded boundary.

If in the time-independent plasticity case, the material exhibits a "yield" strength at high stresses (stress to give infinite strain rate), then provided that the yielded zone is small in comparison with the crack length, eqns (1) and (20) combine to give

$$\dot{\delta}=\phi(n)\frac{\dot{\epsilon}_0}{\sigma_0{}^n}\frac{1}{\sigma_y}\frac{2}{(n+1)}\sigma^{n+1}\pi a. \tag{22}$$

This model assumes that the deviation of the stresses in the "yield" zone from the non-linear elastic stresses, is too small to affect the value of J as given by the energy bound approximation.

COMPARISON WITH OTHER DATA

A comparison with the non-linear finite-element data of Goldman and Hutchinson is included in Fig. 4. As their results were given for *finite*-width plates, the data for the smallest ratio of internal crack length to plate width (1/8) were semi-empirically corrected to represent an infinite plate, by dividing the results by the usual linear-elastic width correction raised to the power $(n+1)$.

However in comparing the finite element data with the upper-bound, it should be noted that the former describes uniaxial loading of the plate whereas the latter is for biaxial loading and therefore a close relationship may not be obtained.

Although there is no barrier in principle to the formulation of an approximate stress field for uniaxial loading based on Inglis equations and Sih's correction stress function, the equations become extremely lengthy and require to be cast in complex form. Trials of the shorter biaxial formulation in complex form showed that the computer time increased enormously due to the complex arithmetic and therefore the uniaxial solution has not been attempted so far.

Nevertheless, it can be shown from Inglis equations that a greater volume of material at a crack tip reaches a given $\bar{\sigma}$ under uniaxial plane strain than under biaxial plane strain[26]. Hence it may be argued that the uniaxial plane strain results should indeed fall above the exact biaxial plane strain results.

Comparison has also been made in Fig. 5 with Gildfind's experimental results obtained on double-edge cracked plates. The test specimens were thin enough to be suffering plane stress and the loading was uniaxial. The constitutive relation was varied from $3 > n > 11$ by altering the material and/or the prior heat treatment of the specimens. J was inferred from crack tip-opening-displacement measurements through a relation similar to eqn (3) which also incorporated a semi-empirical geometric correction factor. For the present comparison, the original geometric correction was removed, and alternative corrections substituted. The first has been referred to earlier and for the second, Goldman and Hutchinson's results were used with the further addition of a factor to increase the correction from the internal crack case to the edge crack geometry. The comparison is shown in Fig. 4 where the upward pointing symbols

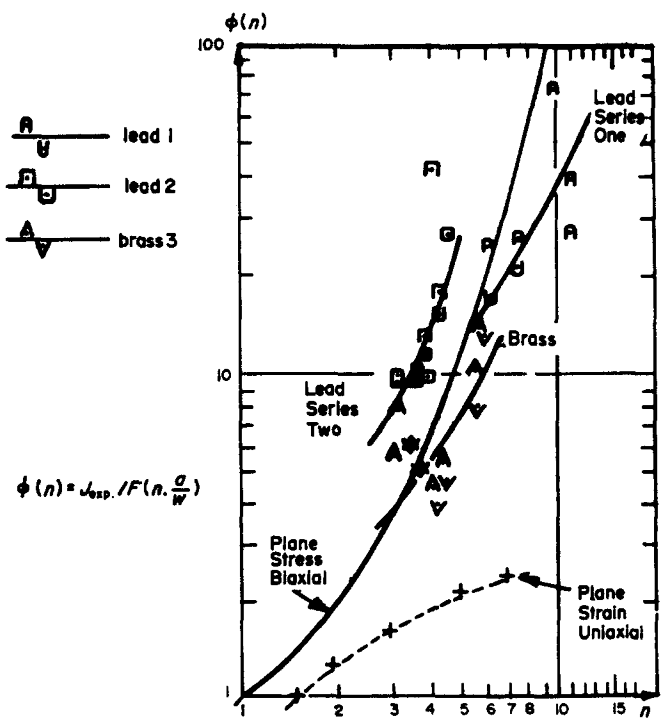

Fig. 5. Comparison with Gildfinds results.

(e.g. ∩) refer to the first form of correction and the inverted symbols (∪) refer to Goldman and Hutchinson's correction.

It is quite clear from this comparison that the multiplying factor increases substantially with n, although the fair agreement in Fig. 5 must be treated as somewhat fortuitous. It should also be emphasised that it is never as simple as it seems to fit material behaviour measurements to simple constitutive laws and therefore the scatter from one material to another is hardly surprising. The constitutive law constants and the experimental values shown, were themselves means of several tests.

NON-LINEAR EQUIVALENT OF THE PLASTIC-ZONE-SIZE CORRECTION FACTOR

One of the most likely reasons for divergence between theory and experiment shown in Fig. 5 is that the details of the constitutive relations exhibited by the materials are probably inadequately described in the analysis. In most materials which follow an n-power law for part of their loading curve, a point will usually be reached at high stresses where the strains or the strain rates tend to infinity ($n \to \infty$). For example, in some polymers the creep index increases with stress and a fixed n-power law can only be ascribed to a limited range of applied stress.

It might be more realistic for such cases to visualise a perfectly-plastic crack-tip zone where the stress is uniform, namely, a specified "yield" value σ_Y, the plastic zone being embedded in a non-linear field. (This model applies equally to non-linear plasticity or to creep, as perfect-plasticity and infinite creep rate cannot be distingushed.) Alternatively the crack tip zone could be modelled in terms of a higher n-power dependence than the main body of the material. These models are shown in Fig. 6.

The rigorous solution of such models appears difficult—for example, the classical Dugdale Model route would be frustrated by the absence of point-force factors for non-linear bodies and by the invalidity of the superposition principle. However, the approximate plastic zone size treatment of Irwin[27] is no less logical when applied to non-linear materials. Therefore taking the near-crack-tip stress distribution normal to the crack plane as given by Hutchinson[5], we obtain

$$\sigma_y = \alpha(n)\left[\frac{J}{\epsilon_0/\sigma_0{}^n}\right]^{1/(n+1)} \frac{1}{(2\pi r)^{1/n+1}} \tag{23}$$

(where α is a function of α tabulated by Hutchinson) setting $\sigma_y = \sigma_Y$,

$$r_Y = \frac{\alpha^{n+1}}{2\pi(\epsilon_0/\sigma_0{}^n)}\cdot\frac{J}{\sigma_Y{}^{n+1}} \tag{24}$$

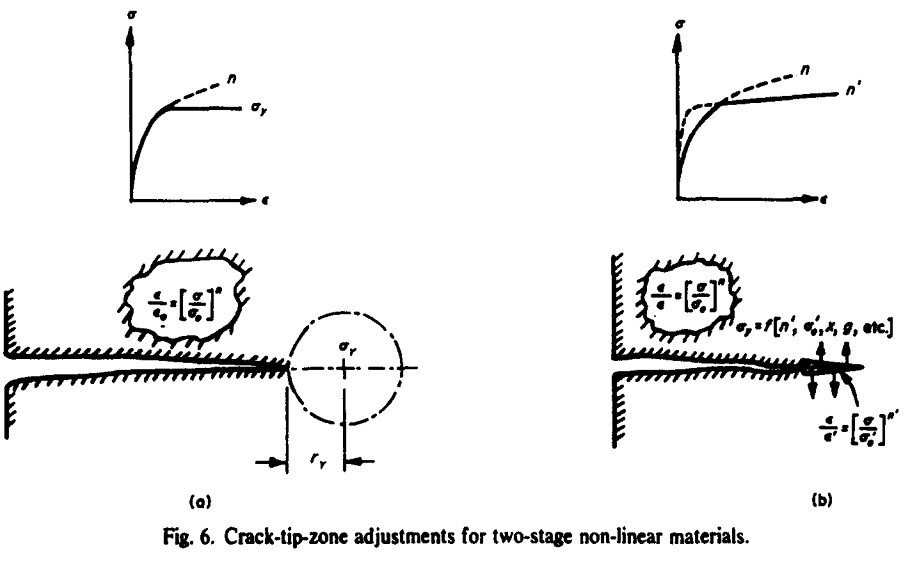

Fig. 6. Crack-tip-zone adjustments for two-stage non-linear materials.

or in terms of the present upper bound approximation

$$r_Y = \frac{\propto^{n+1}}{2\pi(\epsilon_0/\sigma_0{}^n)}\phi(n, a/W)\left(\frac{\sigma}{\sigma_Y}\right)^{n+1}\pi a. \tag{25}$$

Alternatively, for the "non-linear" plastic zone model of Fig. 6(b), an equivalent yield stress can be found by comparing eqns (1) and (3) whence

$$\sigma_Y = \frac{\sigma_0{}^{(n'-1)/n'}}{(\epsilon_0{}'g)^{1/(n'+1)}}\cdot\left(\frac{n'+1}{n'}\right)^{n'/(n'+1)}\left[\phi(n)\frac{\epsilon_0}{\sigma_0{}^n}\cdot\frac{2}{(n+1)}\cdot\pi a\right]^{1/(n'+1)}\sigma^{(n+1)/(n'+1)}. \tag{26}$$

Insertion of eqn (25) into (24) allows the determination of a notional plastic zone size which can be added to the real crack length. This method of evaluation r_Y could also be used to index triaxial state by comparison with plate thickness. It is however questionable to what extent gross plasticity or creep is compatible with the maintenance of plane strain, especially if crack-tip blunting occurs.

It is clear from eqn (25) that the intervention of perfect plasticity has a marked effect as r_Y is proportional to ϕ which in turn increases sharply with n. However there is an offsetting effect relative to the linear-elastic experience in that the dependence on σ/σ_Y reduces as n increases. This circumstance arises because the difference between the perfectly-plastic crack tip stress pattern and the non-linear distribution is less than for the linear elastic case. Therefore the relaxation of high crack-tip stresses disturbs the overall stress pattern less.

SUMMARY AND CONCLUSION

Plane strain and plane stress upper bound analyses have been given for a classical Griffith crack in a body made of entirely non-linear plastic or creeping material. The analyses can be changed with little trouble to describe constitutive laws other than the single n-power law used in the present study. Values of J or $\dot{J}$ have been given $0.1 < n < 14$.

Comparison with other relevant data has been made, and although there are some areas of doubt, particularly with regard to finite-width effects, the general form of the upper bound results seem correct. The results may be considered significant and applicable in the following respects:

1. If the nominal stress applied to the cracked body is sufficient to produce a gross strain field which is dominated by a high n-power monotonic or creep law, J or $\dot{J}$ will be greatly underestimated by linear theory.

2. The functional dependence of J is dominated by the n-dependent factor ϕ, and by the applied stress which is raised to the power $(n + 1)$, rather than by the crack length.

3. The analysis permits the estimation of approximate plastic zone sizes which may be useful for establishing crack length adjustments and for indexing triaxial states.

4. Substantial differences have been shown between plane strain and plane stress values of J. Unlike the linear elastic case, the in-plane transverse components of stress have a strong influence on the crack tip stress state.

REFERENCES

1. D. S. Dugdale, *J. Mech. Phys. Solids* **8**, 100 (1960).
2. D. J. Hayes and J. G. Williams, *Int. J. Fract. Mechs.* **8**, 239 (1972).
3. J. R. Rice and G. F. Rosengren, *J. Mech. Phys. Solids* **16**, 1 (1968).
4. J. W. Hutchinson, *J. Mech. Phys. Solids* **16**, 13 (1968).
5. J. W. Hutchinson, *J. Mech. Phys. Solids* **16**, 337 (1968).
6. J. W. Hutchinson, *J. Appl. Mechs.* **35**, 379 (1968).
7. N. J. Hoff, *Quart. Appl. Math.* **12**, 49 (1954).
8. J. A. Begley and J. D. Landes, Fracture toughness. *Proc.* 1971 *Nat. Symp. on Fract. Mechs. ASTM STP* **514**, 24 (1972).
9. P. A. Gildfind, PhD Thesis, University of Strathclyde, Glasgow (1972).
10. N. L. Goldman and J. W. Hutchinson, *Int. J. Solids Structures* **11**, 575 (1975).
11. K. M. Nikbin, G. A. Webster and C. E. Turner, Cracks and fracture. *ASTM STP* **601**, 47 (1976).
12. J. R. Rice, *Rep. E39, ARPA SD* 86, Brown University (1967).
13. H. W. Hayden, W. G. Moffat and J. Wulff, *The Structures and Properties of Materials*, Vol. 3. Wiley, New York (1965).
14. J. E. Goddon, *The New Science of Strong Materials.* Penguin Books, Harmondsworth, England (1973).
15. J. Knott, *Fundamentals of Fracture Mechanics.* Butterworths, London (1973).
16. F. K. G. Odqvist, *Mathematical Theory of Creep and Creep Rupture.* Oxford University Press (1974).

17. I. Finnie and W. R. Heller, *Creep of Engineering Materials*. McGraw-Hill, New York (1959).
18. A. A. Ilyushin, *PMM* **10**, 347 (1946).
19. A. C. Stevenson, *Phil. Mag. VII* **36**, 178 (1945).
20. C. E. Inglis, *Trans. Inst. Nav. Archs.* **55**, pt 1, 219 (1913).
21. S. Timoshenko and J. N. Goodier, *Theory of Elasticity*. McGraw-Hill, New York (1951).
22. A. A. Griffith, *Phil. Trans. Roy. Soc. London* **A221**, 163 (1921).
23. A. A. Griffith, *Proc. 1st Int. Cong. for App. Mechs.*, p. 55, Delft, Netherlands (1924).
24. A. J. M. Spencer, *Int. J. Engng Science* **3**, 441 (1965).
25. G. C. Sih and H. Liebowitz, *Int. J. Solids Structures* **3**, 1 (1967).
26. T. G. F. Gray, PhD Thesis. University of Strathclyde, Glasgow (1978).
27. G. R. Irwin, *Seventh Sagamore Ordnance Materials Res. Conf.* Washington DC, US Office of Tech. Services (1961).

APPENDIX

Defining stresses at a point in elliptical coordinates as the differences between the stresses given by the Inglis solution and the solution for a uniform radial boundary traction of σ at a large outer boundary ξ_{max} as $\Delta\sigma_\eta$, $\Delta\sigma_\xi$, $\Delta\tau_{\eta\xi}$

$$\Delta\sigma_\eta + \Delta\sigma_\xi = \sigma\frac{2\cosh^2\xi_0(1+\tanh\xi_0)^2}{(\cosh 2\xi_{max} + \cos 2\eta)}\left[\frac{(1+m^2)}{2} - \frac{3m(\cosh 2\xi\cos 2\eta + 1)}{(\cosh 2\xi_{max} + \cos 2\eta}\right] \tag{27}$$

$$\Delta\sigma_\eta - \Delta\sigma_\xi + 2i\tau_{\eta\xi} = \sigma\frac{2\cosh^2\xi_0(1+\tanh\xi_0)^2}{(\cosh 2\xi_{max} + \cos 2\eta)}\left[2m - \frac{3m(\cosh 2\xi\cos 2\eta + 1)}{(\cosh 2\xi_{max} + \cos 2\eta)}\right]\times(\cos\omega + i\sin\omega) \tag{28}$$

where

$$m = \frac{1-\tanh\xi_0}{1+\tanh\xi_0}$$

$$\cos\omega = \frac{\cosh 2\xi\cos 2\eta - 1}{\cosh 2\xi - \cos 2\eta}; \qquad \sin\omega = \frac{\sinh 2\xi\sin 2\eta}{\cosh 2\xi - \cos 2\eta}$$

ξ_{max} = outer boundary, where $\sigma_\xi = \sigma$, ($R \simeq \cosh\xi_{max}$)